Controlling femtosecond-laser-driven shock-waves in hot, dense plasma

Amitava Adak[1], Prashant Kumar Singh[1], David R. Blackman[2], Amit D. Lad[1], Gourab Chatterjee[1], John Pasley[2,3], A. P. L. Robinson[3],G. Ravindra Kumar[1a)]

[1)] *Tata Institute of Fundamental Research, Dr. Homi Bhabha Road, Colaba, Mumbai-400005, India*

[2)] *York Plasma Institute, University of York, Heslington, York YO10 5DQ, United Kingdom*

[3)] *Central Laser Facility, Rutherford-Appleton Laboratory, Chilton, Didcot OX10 0QX, United Kingdom*

(Dated: 15 August 2017)

Ultrafast pump-probe reflectometry and Doppler spectrometry of a supercritical density plasma layer excited by $10^{17} - 10^{18}$ W/cm^2 intensity, 30 fs, 800 nm laser pulses reveal the interplay of laser intensity contrast and inward shock wave strength. The inward shock wave velocity increases with an increase in laser intensity contrast. This trend is supported by simulations as well as by a separate independent experiment employing an external prepulse to control the inward motion of the shock wave. This kind of cost-effective control of shock wave strength using femtosecond pulses could open up new applications in medicine, science, and engineering.

I. INTRODUCTION

Contemporary experiments on intense, ultrashort laser driven shock waves in condensed media offer exciting opportunities for mimicking hot, dense scenarios in intrastellar and intraplanetary environments[1]. High pressures in the megabar regime have been created before in solid state science experiments using diamond anvil cells under static conditions[2]. However, these cells cannot withstand temperatures higher than a few thousand kelvin. On the other hand, creation of high energy density plasmas in the laboratory is possible by virtue of intense laser-solid interactions[1,3] which can lead to the realization of dynamic compression of the material achieving much higher pressures than those in diamond anvil cells[2]. The technique of chirped pulse amplification[4] produces intense ultrashort laser pulses on a table top and has spurred controllable exploration of 'extreme conditions' of matter[5–17]. The temporal dynamics of ultrashort laser-plasma interactions have just begun to be explored in overdense and near solid density plasma[10–12]. An important aspect of this high energy density science is the creation of laser-driven shock waves. However, more than the shock wave itself, it is the control of the shock wave that plays an important role in many studies[18–20]. Therefore, it is important to have techniques for enhancing the shock strength that do not involve expensive pulse shaping techniques or specific target characteristics. In an interesting and exciting parallel, a recent proposal seeks to produce coherent terahertz radiation by shock waves in crystalline polarizable materials[18], which has great potential for applications in industry, geophysics and medicine[20].

In this paper we demonstrate control of femtosecond-laser-driven shock waves by changing a single parameter of the laser pulse namely, its intensity contrast (peak to pedestal intensity ratio). Typically, relativistic intensity femtosecond pulses have peak intensities above 10^{18} W/cm^2 but have significant intensity a few picosecond before the incidence of the peak intensity on a target. Recent technology has improved this peak to picosecond contrast from less than 10^5 to greater than 10^8 at current levels. Many phenomena observed at low-contrast have been revisited with high-contrast pulses[21–23] but little work has been done on the creation and propagation of shock waves produced by ultrashort laser pulses as the contrast improves. To demonstrate that shock waves can be controlled by modifying the prepulse in such short pulse interactions, we present measurements of the picosecond resolved reflectivity and Doppler shift of a probe pulse that interrogates the plasma produced by the high intensity laser pulse (10^{18} W/cm^2). We choose a high electron density ($\sim 10^{22}$ cm^{-3}) layer in the plasma for such probing by using a 266 nm probe pulse, generated from the fundamental (pump) laser pulse at 800 nm. In our study, we use two independent laser systems, one with a contrast of 10^5 and another with a contrast of 10^7, 50 ps before the incidence of peak intensity.

The effect of increasing contrast is clearly seen in the sharper rise of reflectivity of a second harmonic (400 nm) probe. For high-contrast (10^7), Doppler spectrometry at 266 nm shows 10 times faster inward motion of a super-critical ($n_{cr-probe} = 1.6 \times 10^{22}$ cm^{-3}) surface than that observed in our earlier experiment[12] with a low-contrast (10^5) laser indicating shock strength enhancement. Moreover, by varying the pre-plasma scale-length with an external prepulse we show that the amplitude of the red shift observed in the spectrum of the emitted second harmonic of the pump is larger for short plasma scale-length (or high-contrast laser) than it is for long plasma scale-length (or low-contrast laser). In this paper, we introduce the opportunity of manipulating a femtosecond-laser-driven shock wave using a relatively inexpensive approach that is not target specific. This study opens up the opportunity to generate coherent terahertz radiation[18,19,24] at desired frequencies by using the con-

[a)] Electronic mail: grk@tifr.res.in

trollable shock wave velocity to induce a periodic oscillations in the static polarization inside a crystalline polarizable material.

II. EXPERIMENTAL SETUP

The experiment was performed at the Ultrashort Pulse High Intensity Laser Laboratory (UPHILL), at the Tata Institute of Fundamental Research, Mumbai using two Ti:Sapphire lasers ($\sim$ 800 nm, 30 fs) having different intensity contrasts (inset of Fig. 1(a)). A polished dielectric slab (BK7 glass) was irradiated by the main pump pulse focussed by a gold coated off-axis parabolic mirror in $\sim$ f/4 geometry at 45^0 angle of incidence. A small fraction of the pump pulse was split off and up-converted to its second harmonic ($\sim$ 400 nm) and third harmonic ($\sim$ 266 nm) to probe the plasma dynamics. The probe is passed through a retroreflector mounted on a micron precision delay stage. This probe pulse was then focused on the interaction region and its specular reflection was collected by a lens to (i) a photodiode for reflectivity studies and (ii) a high resolution spectrometer for Doppler spectrometry. The shot-to-shot fluctuation of the laser intensity was found to be less than 6%. The spot size of the focused pump-pulse on the target was $\sim$ 14 μm (FWHM).

III. CONTRAST DEPENDENT REFLECTOMETRY

The level of laser intensity contrast is inherently coupled to the pre-plasma scale-length. In order to see the inference of the pre-plasma with different laser contrast, a time-resolved pump-probe reflectometry experiment was carried out. Figure 1(a) shows the temporal behaviour of the reflected second harmonic ($\sim$ 400 nm) probe pulse (probing density up to $\sim 7\times10^{21}$ cm^{-3}) from the plasma created in two independent experiments using the high and low-contrast lasers (inset of Fig. 1(a)) at similar peak intensities of $\sim 2 \times 10^{17}$ W/cm^2. The reflectivity rise for the high-contrast laser is more pronounced than that for the low-contrast one. Analysis of the reflectivity curves show that the slope of the rising reflectivity is steeper (0.5 ± 0.1 ps^{-1}) in the former case than in the latter case (0.3 ± 0.1 ps^{-1}). The FWHMs of the reflectivity spikes in these two cases are 1.8 ± 0.4 ps and 2.8 ± 0.5 ps respectively. The higher probe reflection at pump arrival, can be qualitatively described by simple models for the pump interaction (resonance absorption) and the probe absorption in the hot dense plasma that is created. Since the pre-plasma scale-lengths in our experiments are on the falling side of the resonance absorption vs scale-length curve[25], the high-contrast laser is absorbed more via efficient resonance absorption (hotter plasma formation) than the low-contrast laser. Therefore, the normally incident probe for the high-contrast pump will be absorbed less (higher reflectivity) at that early time in hotter plasma with shorter scale-length by inverse bremsstrahlung[25]. On the other hand, at longer temporal delays of 10's of picosecond, there is more rapid plasma expansion due to the higher initial temperature. This implies that the plasma scale-length will be longer at that longer temporal delays for the high-contrast laser and will lead to enhance probe absorption (and hence less reflection) than in the other case.

IV. DOPPLER SPECTROMETRY WITH THIRD HARMONIC PROBE

The blue curve in the inset of Fig. 1(a) shows the laser intensity contrast used for the time-resolved pump-probe Doppler spectrometry experiment. The results from this experiment (10^7 contrast) are compared (Fig. 1(b)) to those from our earlier experiment[12] performed with a contrast of 10^5 (red curve in the inset of Fig. 1(a)). The time-resolved Doppler shifts with the high-contrast laser, are shown in Fig. 1(b) by blue circles (the pump pulse energy of 90 mJ) and those measured in the earlier study[12] are multiplied by 10 (black square). An order higher wavelength shifts for the high-contrast laser imply that the plasma dynamics in this case are more rapid i.e. the critical density layer of the probe moves much faster. The early time red shifts are due to the inward propagation of a shock wave. Therefore, in the present study, a shock wave with a much higher velocity is observed than in the earlier one.

A simple analysis of a 1-D, isolated strong shock wave in an ideal fluid shows that the maximum shocked fluid density is 4 times higher than the upstream density[1]. This simple estimate indicates that a strong shock wave can produce a maximal plasma density (n_m) of the order of $4n_e$ (n_e being the local upstream plasma density). However, additional ionisation caused by the passage of the shock wave can increase this density further. At very early time when the shock wave is propagating across the critical density (of the pump) towards the overdense region, the third harmonic probe transmits through the shocked plasma as long as the density of the shocked plasma is sub-critical for the ultraviolet probe (this happens until the shock wave climbs upto an upstream density, where $n_m \sim n_{cr-probe}$). During this early period, the probe is momentarily reflected from the expanding unshocked plasma in the upstream region giving rise to a transient blue shift in the Doppler measurement (Fig. 1(b)). Earlier measurements[12] lacked early time data and could not capture this transient blue shift. However, detailed dynamics in this early time period are fairly complicated and need more exploration. As soon as the shocked plasma density becomes overcritical for the probe, it becomes reflective and the probe gets redshifted thereafter until the shock wave penetrates beyond the overcritical region (for the probe). Thereafter, the probe again reflects from the expanding plasma density gradient giving rise to a sustained blue shift. Whilst the

scaling of pressure with laser intensity is still expected to follow a roughly $I^{0.66}$ scaling (assuming other parameters are unchanged), the scaling of shock velocity with intensity is non-trivial, being dependent on the details of the material EOS.

V. SIMULATION

To compare the physical mechanism producing the shock waves observed in both the experiments with low (Adak *et al.*[12]) and high-contrast lasers, numerical simulations for both situations are compared. In both cases, HYADES[26], a 1-D Lagrangian radiation-hydrodynamics simulation code incorporating multi-group radiation diffusion and a flux-limited diffusion model of electron conduction, is used to model the interaction of the pump laser pre-pulse with the initially solid BK7 glass target. Accurately modelling the pre-plasma formation requires an accurate prepulse laser-intensity profile. The intensity profile is set at a fixed level ($10^{-5}I_{max}$ for low-contrast and $10^{-7}I_{max}$ for high-contrast) for the first 475 ps, with the last 25 ps of the 500 ps pre-pulse modelled using a piecewise linear fit to the laser contrast measurements from the two experiments (see the inset of Fig. 1(a)) to accurately represent the shape of the pre-pulse whilst removing the high frequency noise present in the measurement.

To model the main pulse interaction the density profile, temperature and ionisation data from HYADES are used to initialise a 1D particle-in-cell (PIC) code ELPS[27]. The perturbation obtained from the PIC code is then used in a simple 1D hydrodynamic model to calculate the formation and evolution of shock-wave like perturbations later in time. This 1D hydrodynamic model involves a 1D compressible fluid code, without radiation transport. It solves the Euler equations in 1D assuming an ideal gas equation of state and without thermal conduction. Figure 2(b) shows the comparison of the experimental observations (velocity of the probe-critical surface) from the low-contrast laser-plasma interaction in Ref.[12] to the results of the serial hydro-PIC-hydro calculations. Similarly Fig. 2(a) shows a comparison of the results with the high-contrast laser. For a full discussion of the mechanism producing the shock waves, see Ref.[12].

The later behaviour of the target, including the formation and evolution of a shocked layer within the target, appear to be well explained by hydrodynamic models, as evidenced by the good quality match with the experimental observations at these times. In addition to this, the initial expansion of the target appears to be well modelled by HYADES.

Figure 3 shows the electron density profile for the pre-plasma just before the main pulse interaction in both experiments. The region around the critical density (e.g. between the n_{crit} and $0.1n_{crit}$ surface) is $\sim$ 4 times smaller in the high-contrast pre-plasma compared to the low-contrast regime. The significantly reduced mass of the interaction region, leads to an increase in energy density. The low-density scattering of laser light away from the target in the high-contrast case is reduced and a greater change in ionisation occurs here also due to the material being initially colder. These factors combine to produce very much steeper pressure gradients and greatly enhanced acceleration in the high-contrast case, leading to the dramatic enhancement in shock velocity that is observed in the experiment.

Due to the differing limitations of the hydrodynamics codes available to us we performed the final stage of the modelling (the post-pulse hydrodynamic evolution) with two different codes, in parallel efforts. Firstly we performed modelling using a simple 1D compressible fluid code which was written so as to enable the mean ion velocity in different regions from the PIC calculation, as imparted by the main pulse, to be transferred to the hydrodynamic code alongside information pertaining to thermal energy deposition. This code however, does not enable the use of a non-ideal gas EOS, so does not capture the shock wave propagation adequately. Therefore HYADES was also employed to simulate this final stage of the evolution, with the limitation here that the main pulse was mimicked only by matching the energy deposited in a given region as given by the PIC code. The findings of both these modelling efforts support the conclusions described in this manuscript, and the main discrepancy between the two was a 2 ps delay in shock formation in the HYADES case.

To show the progression of the shock waves produced by the main pulse interacting with the pre-plasma, energy density profiles produced by the PIC code runs described earlier were used as the basis for this further HYADES calculations. Figure 4 shows the shock waves traversing past the initial front surface of the targets. The low-contrast simulation (a) showed that the shock wave does not meet the bulk material until much later in time, this is due to the greater level of ablation from the higher intensity pre-pulse. The high-contrast laser pulse (b) on the other hand appears to produce a shock with considerably higher pressure and travelling at higher speed, than in the low-contrast case. The density ratio in the low-contrast shock shows a compression grow from 0.5 to 2.0 between $t = 2$ ps and $t = 10$ ps, whilst the density ratio in the high-contrast case reaches around 10x due to its greater initial strength, ionisation of the cold material at the shock front, and coalescence with the prepulse launched shock front that preceded it into the target.The shock wave is non-stationary due to the short duration of the driver pulse and the small focal spot diameter and so will decay substantially in strength as it propagates further into the target.

It is important to note that any 2D effects are not modelled by the codes employed in this work. Since we are making observations near to the original solid surface, over timescales of a few tens of ps, and given that the pump and probe critical surfaces are only separated by a few microns, we are in a situation where the longitu-

dinal scale is significantly less than the transverse length scale. Therefore, the 1D models can be effectively used to interpret the experiment.

VI. SCALE-LENGTH DEPENDENT DYNAMICS OF THE PUMP-CRITICAL SURFACE

In a separate independent approach, we infer the effect of laser contrast on the strength of shock waves by manipulating the pre-plasma scale-length with an external prepulse. For independent verification we carried out a two-pulse experiment using the laser with 10^7 contrast. A weak external prepulse (100 fs, I $\sim 1\times10^{14}$ W/cm^2) was used to control the plasma scale-length, prior to the arrival of the strong pump pulse (30 fs, I $\sim 1\times10^{18}$ W/cm^2). The time delay between these two pulses was varied, which essentially changes the scale-length of the interaction. Doppler shifts in the harmonics, generated at the pump critical surface, can help in monitoring the motion of the pump critical surface[28]. A spectrometer was used to capture the second harmonic emission in the specular direction of the pump. Scale-length dependent shifts in the emitted second harmonic are shown in Fig. 5. For longer prepulse delay, the spectrum of the emitted harmonic progressively shifts towards the blue side. The plasma scale-length set up by an external prepulse, arriving at different time, was estimated by the MULTI-FS hydrodynamic code[29]. This observation further substantiates our interpretation of the pump-probe Doppler measurements (Fig. 1(b)) performed under two contrast levels, where much higher red shift are observed in the case of high-contrast (or small pre-plasma scale-lengths). The role of an external prepulse is primarily to set up the plasma scale-length, before the arrival of the main pulse, and therefore to control the energy density near the critical-density region. The external prepulse of intensity $\sim 10^{14}$ W/cm^2, alone is not strong enough to launch shock waves of the strength observed in the experiment. The application of the external prepulse allows the pre-plasma conditions to be systematically varied, leading to significant changes in the conditions produced by the absorption of the main pulse, thereby affecting the strength of the shock wave produced.

VII. CONCLUSION

In conclusion, we have shown that the inward shock wave velocity increases by an order of magnitude with an increase in laser intensity contrast from 10^5 to 10^7. This result is well reproduced by numerical simulations. The shock wave generation by the main pulse is for the most part driven by the pressure profiles set up by the laser-driven hot electron energy deposition, as modelled by the PIC code. This pressure profile results in the fluid being accelerated and, over time, the formation of a shock wave. For the high contrast case i.e. for the steeper density gradient the laser energy deposition happens in region that is both less massive and thinner (compared to the lower contrast case) leading to a higher energy density and stronger shock formation. Furthermore, by an independent experiment with external prepulse we have shown a control over the inward motion of the shock wave velocity by manipulating the pre-plasma density scale-length. Therefore by controlling the laser contrast or pre-plasma scale-length, it is possible to manipulate the femtosecond-laser-driven shock wave velocity, which could lead to many potential applications in medicine, engineering, and science[18,19,24,30].

VIII. ACKNOWLEDGEMENTS

GRK acknowledges a J.C. Bose Fellowship grant.

[1] R. P. Drake, *High Energy Density Physics* (Springer-Verlag, Berlin, Heidelberg, 2006).
[2] R. F. Smith J. H. Eggert, R. Jeanloz, T. S. Duffy, D. G. Braun, J. R. Patterson, R. E. Rudd, J. Biener, A. E. Lazicki, A. V. Hamza, J. Wang, T. Braun, L. X. Benedict, P. M. Celliers, and G. W. Collins, Nature **511**, 330-333 (2014).
[3] P. Gibbon, *Short Pulse Laser Interactions With Matter* (Imperial College Press, 2005).
[4] D. Strickland and G. Mourou, Opt. commun. **55,** 447 (1985).
[5] X. Liu and D. Umstadter, Phys. Rev. Lett. **69,** 1935 (1992).
[6] A. Ng, P. Celliers, A. Forsman, R. M. More, Y. T. Lee, F. Perrot, M. W. C. Dharma-wardana, and G. A. Rinker, Phys. Rev. Lett. **72**, 3351 (1994).
[7] P. Gibbon and E Forster, Plasma Phys. Control. Fusion **38**, 769-793 (1996).
[8] A. S. Sandhu, G. R. Kumar, S. Sengupta, A. Das, and P. K. Kaw, Phys. Rev. Lett. **95**, 025005 (2005).
[9] S. Kahaly, S. K. Yadav, W. M. Wang, S. Sengupta, Z. M. Sheng, A. Das, P. K. Kaw, and G. R. Kumar, Phys. Rev. Lett. **101**, 145001 (2008).
[10] S. Mondal, A. D. Lad, S. Ahmed, V. Narayanan, J. Pasley, P. P. Rajeev, A. P. L. Robinson, and G. R. Kumar, Phys. Rev. Lett. **105,** 105002 (2010).
[11] Y. Ping, A. J. Kemp, L. Divol, M. H. Key, P. K. Patel, K. U. Akli, F. N. Beg, S. Chawla, C. D. Chen, R. R. Freeman, D. Hey, D. P. Higginson, L. C. Jarrott, G. E. Kemp, A. Link, H. S. McLean, H. Sawada, R. B. Stephens, D. Turnbull, B. Westover, and S. C. Wilks, Phys. Rev. Lett. **109,** 145006 (2012).
[12] A. Adak, D. R. Blackman, G. Chatterjee, P. K. Singh, A. D. Lad, P. Brijesh, A. P. L. Robinson, J. Pasley, and G. R. Kumar, Phys. Plasma **21,** 062704 (2014).
[13] A. Adak, P. K. Singh, A. D. Lad, G. Chatterjee, M. Dalui, P. Brijesh, A. P. L. Robinson, John Pasley, and G. R. Kumar, Appl. Phys. Lett. **109,** 174101 (2016).
[14] S. Mondal, V. Narayanan, W. J. Ding, A. D. Lad, B. Hao, S. Ahmad, W. M. Wang, Z. M. Sheng, S. Sengupta, P. Kaw, A. Das, and G. R. Kumar, Proc. Natl. Acad. Sci. **109,** 8011 (2012).
[15] P. K. Singh, G. Chatterjee, A. Adak, A. D. Lad, P. Brijesh, and G. R. Kumar, Optics Express **22**, 22320 (2014).
[16] G. Chatterjee, P. K. Singh, A. Adak, A. D. Lad, and G. R. Kumar, Rev. Sci. Instrum. **85,** 013505 (2014).
[17] A. Adak, A. P. L. Robinson, P. K. Singh, G. Chatterjee, A. D. Lad, J. Pasley, and G. R. Kumar Phys. Rev. Lett. **114**, 115001 (2015).
[18] E. J. Reed, Michael R. Armstrong, Kiyong Kim, Marin Soljai, Richard Gee, James H. Glownia, John D. Joannopoulos, Materials Today **10**, 44-50 (2007).
[19] E. J. Reed, Marin Soljacic, Richard Gee, and J. D. Joannopoulos, Phys. Rev. Lett. **96**, 013904 (2006).

[20]K. Takayama and T. Saito, Annu. Rev. Fluid Mech. **36**, 347 (2004).
[21]M. Cerchez, R. Jung, J. Osterholz, T. Toncian, O. Willi, P. Mulser, and H. Ruhl Phys. Rev. Lett. **100**, 245001 (2008).
[22]L. M. Chen, M. Kando, M. H. Xu, Y. T. Li, J. Koga, M. Chen, H. Xu, X. H. Yuan, Q. L. Dong, Z. M. Sheng, S. V. Bulanov, Y. Kato, J. Zhang, and T. Tajima Phys. Rev. Lett. **100**, 045004 (2008).
[23]B. Dromey, M. Zepf, A. Gopal, K. Lancaster, M. S. Wei, K. Krushelnick, M. Tatarakis, N. Vakakis, S. Moustaizis, R. Kodama, M. Tampo, C. Stoeckl, R. Clarke, H. Habara, D. Neely, S. Karsch, and P. Norreys Nat. Phys. **2**, 456 (2006).
[24]M. R. Armstrong,Evan J. Reed, Ki-Yong Kim, James H. Glownia, William M. Howard, Edwin L. Piner, and John C. Roberts, Nat. Phys. **5**, 285-288 (2009).
[25]W. L. Kruer, *The physics of laser plasma interactions* (Boulder, Colorado, 2003).
[26]HYADES is a commercial product of Cascade Applied Sciences. Email: Larsen@casinc.com.
[27]A. P. L. Robinson, R. M. G. M. Trines, J. Polz, and M. Kaluza. Plasma Phys. Controlled Fusion **53**, 065019 (2011).
[28]M. Zepf, M. CastroColin, D. Chambers, S. G. Preston, J. S. Wark, J. Zhang, C. N. Danson, D. Neely, P. A. Norreys, A. E. Dangor, A. Dyson, P. Lee, A. P. Fews, P. Gibbon, S. Moustaizis, and M. H. Key, Phys. Plasmas **3**, 3242 (1996).
[29]R. Ramis, K. Eidmann, J. Meyer-ter-Vehn, S. Huller, Computer Physics Communications **183**, 637-655, (2012).
[30]D. D. Dlott, Annu. Rev. Phys. Chem. **50,** 251 (1999).

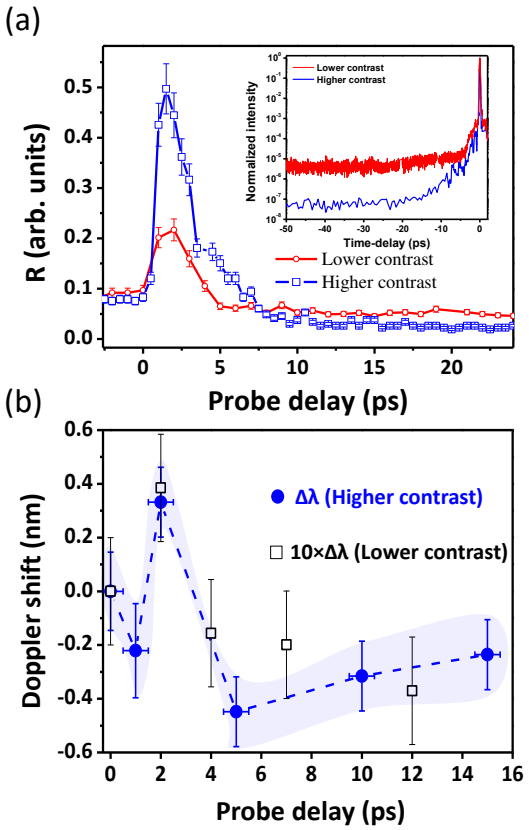

FIG. 1. (a) Comparison of the probe reflectivity from the plasma created by these two lasers in two independent experiments at similar laser intensities of $\sim 2 \times 10^{17}$ W/cm^2. The inset shows temporal intensity profiles of the two femtosecond lasers, measured by a third-order cross-correlator (SEQUOIA). (b) Doppler shifts from the pump-probe Doppler spectrometry experiment using the high-contrast laser (blue circles) shows a clear red shift followed by sustained blue shifts. The Doppler shifts in earlier study with a low-contrast pulse[12] are multiplied by 10 and plotted on the same scale (black squares). The laser peak intensities were $\sim 10^{18}$ W/cm^2.

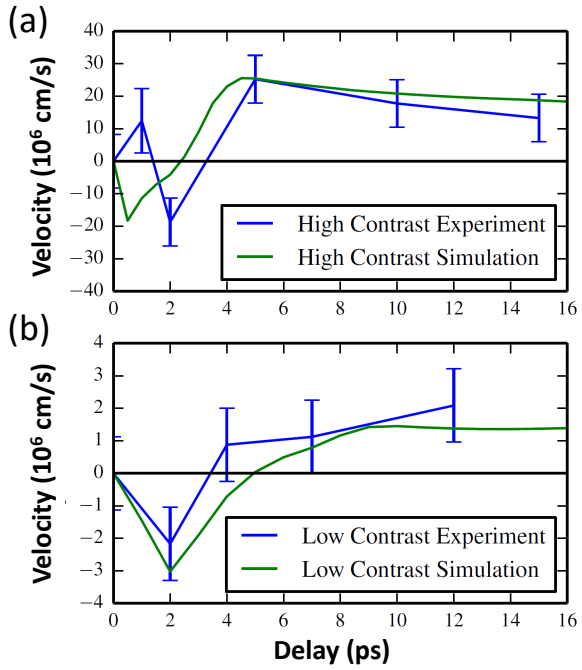

FIG. 2. Comparison of the velocity of the probe-critical surface found in the numerical simulation with observations from (a) high-contrast laser experiment, (b) low-contrast laser experiment[12].

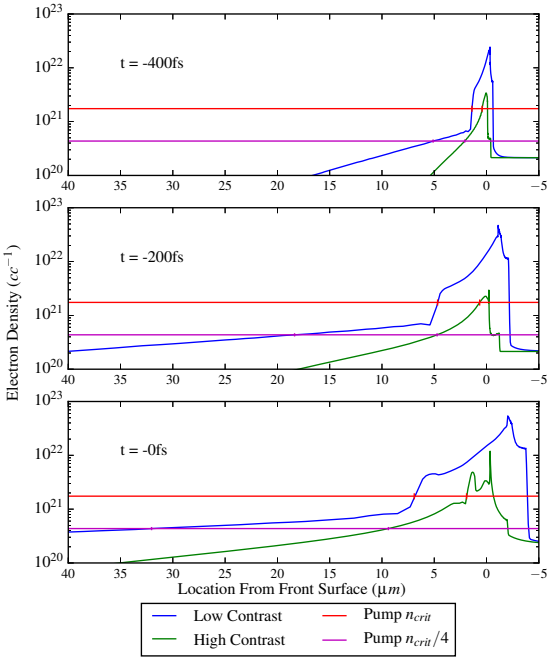

FIG. 3. HYADES results showing electron density profiles for high and low-contrast laser profiles at three time points up to the time of arrival of the main pulse.

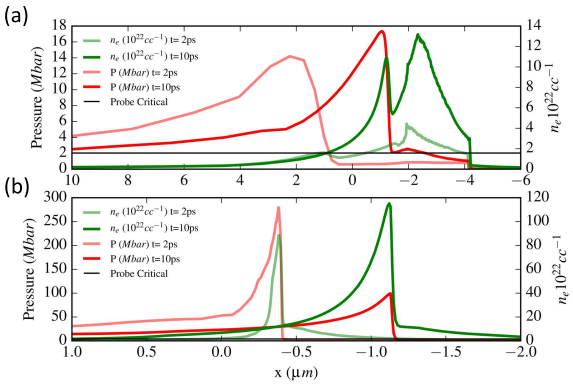

FIG. 4. The pressure and density at later times are shown in both the (a) low-contrast and (b) high-contrast cases taken from coupled PIC-hydrodynamic simulations.

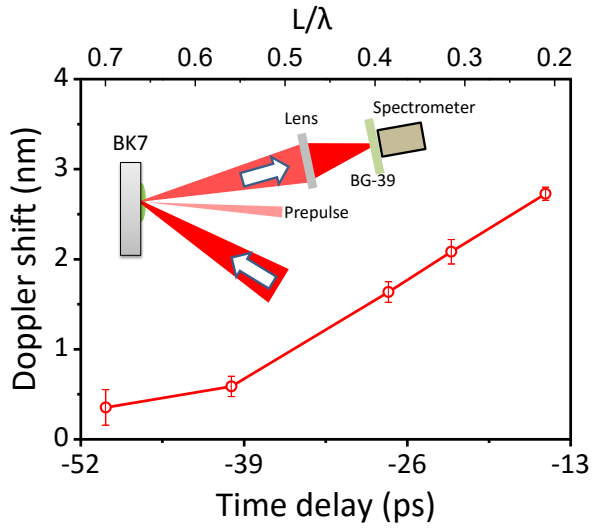

FIG. 5. Scale-length dependent Doppler shift of the emitted second harmonic. The inset shows the experimental set-up using an independent prepulse.